Duplex DNA/Graphene Oxide Biointerface: From Fundamental Understanding to Specific Enzymatic Effects

*Longhua Tang, Haixin Chang, Yang Liu, and Jinghong Li**

The exploration and fabrication of nano-biointerfaces have fundamental significance and practical importance in many fields including chemistry, biology, and materials science. Recently, the integration of DNA with graphene has been substantially advanced. It is well known that single-stranded (ss) DNA can interact with graphene (or graphene oxide) via π–π stacking. However, for the case of DNA duplex/graphene, the studies are still not conclusive. Most work does not address the question of whether or how dsDNA is attracted to graphene oxide (GO). Here the interaction of DNA/GO is systematically investigated and its nanobiological effects, molecular recognition, and biosensing are explored. It is demonstrated that GO can adsorb DNA duplexes, which is possibly facilitated by partial deformation of the double helix on GO. Additionally dsDNA on GO shows specific effects on enzymatic degradation, which could be effectively cleaved by DNA enzyme I and restriction endonucleases as EcoR I, whereas it is highly resistant to degradation by Exo III. An improved understanding of the behavior of these GO/DNA entities will facilitate the development of applications in biomedicine, biosensing, and bionanotechnology.

1. Introduction

Exploration and fabrication of the nano/bio interfaces between nanomaterial and biocomponents have fundamental significance and practical importance in materials science, nanotechnology, biosensing, and biomedicine.[1–6] In the past few years, the integration of biomolecules with nanomaterials has been substantially advanced.[3–6] For example, single-stranded DNA (ssDNA) has been shown to adsorb on carbon nanotubes (CNTs), thereby enhancing the water solubility of CNTs.[7,8] In addition, certain DNA sequences have been selected to wrap on CNTs and then separate metallic CNTs from the semiconductor CNTs.[7] A number of DNA/CNT-based devices have been developed for biosensing and biomedical applications.[9,10]

L. H. Tang, Dr. H. X. Chang, Dr. Y. Liu, Prof. J. H. Li
Department of Chemistry
Beijing Key Laboratory for Microanalytical Methods and Instrumentation
Key Laboratory of Bioorganic Phosphorus Chemistry and Chemical Biology
Tsinghua University
Beijing 100084, P. R. China
E-mail: jhli@mail.tsinghua.edu.cn

DOI: 10.1002/adfm.201102892

Since its discovery in 2004, graphene – regarded as the mother of other carbon nanostructures – has atttracted increasing fundamental and practical interest due to its unique electronic, mechanical, and optical properties.[11–20] To date, the interplay of graphene or its derivative with nano/micrometer-scale biocomponents (DNA, proteins, bacteria and other cells, etc.) has been profoundly investigated; this has stimulated practical applications in the fields of material functionality,[15] self-assembly,[16] molecular recognition,[17] and imaging.[18]

Among these studies, the interaction of DNA with graphene, especially graphene oxide (GO) is of great interest.[15–18] GO is a derivative of graphene containing a variety of oxygen-containing functionalized groups and thereby exhibiting excellent hydrophilicity and processability. Recent work has shown that ssDNA interacts strongly with graphene or GO, while the affinity for double stranded (ds) DNA or well-folded ssDNA is much lower.[17,21] Based on this phenomenon, the application of graphene in biosensing and other bioengineering applications has recently attracted significant research attention. For instance, complexes of ssDNA/GO have been used as novel biomedical and bioassay platforms, with target applications such as nucleic acids, proteins, metal ions, small molecules, and drug-delivery.[17–21] It has been found that aptamer can be well protected by GO from enzymatic cleavage during cellular transit. This finding may be employed in many biological fields, such as DNA and protein analysis, gene and drug delivery, etc.[18,19,22] Moreover, molecular simulations also provide insights into the fundamental interactions between graphene (or GO) and ssDNA. Overall, it is fairly clear that ssDNA readily adsorbs onto graphene and that this is due to non-covalent π-stacking interactions between the hexagonal cells of graphene and the ring structure of nucleobases.[23]

Despite these studies, understanding of the interactions between duplex DNA and graphene still remains elusive. Little is known about how dsDNA is attracted onto graphene. There is some evidence that dsDNA interacts more weakly with graphene than ssDNA, but this has not been quantified.[17–22] Several studies suggest that the hydrophilic nature of the external surface of DNA could preclude favorable interactions with the hydrophobic graphene surface. On the other hand, several reports indicate the hydrogen bonding or van der Waals attractive forces between DNA and graphene would be

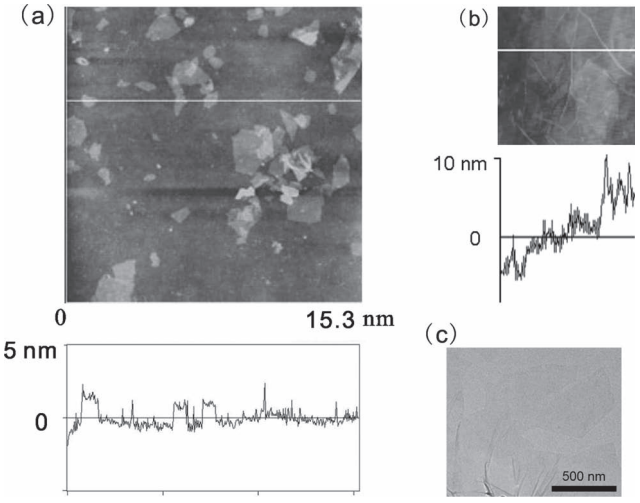

Figure 1. Characterizations of single-layer graphene oxide: a) AFM image and depth profile of graphene oxide on SiO_2 substrate; size 7.0 μm × 7.0 μm; b) AFM image and depth profile of wrinkles on graphene oxide; size 2.0 μm × 2.0 μm; and c) HRTEM image of single-layer graphene oxide. The graphene oxide has ca. 1.2 nm ± 0.2 nm thickness.

sufficient to render the DNA adsorbed on the graphene.[24,25] Recently, Lei et al.[24] reported that dsDNA can bind to GO, forming complexes (dsDNA/GO) in the presence of a high concentration of salts. Zhao et al.[25] used molecular dynamics (MD) simulations to study the interaction of dsDNA segments with the surfaces of graphene and carbon nanotube arrays in aqueous solution. They found that DNA duplexes could self-assemble on the graphene surface by the primary driving force of π-stacking interactions between the ending base pairs of DNA and graphene carbon rings. The simulations, however, do not include counter ions, or charges on the graphene or its derivatives like GO, so that hydrogen bonding and electrostatic forces are not considered. Given the complexity of the systems, it is challenging to probe them by experiment.[24] In order to clarify these controversies and obtain a deeper understanding on dsDNA/GO interactions, specifically on its interaction mechanism, biostability, biological effects, and bioactivity, we carried out a series of experiments to systematically investigate the interaction of DNA/GO, especially between DNA duplex and GO. Surprisingly, we found for the first time that dsDNA also had very strong interactions with GO, which may be facilitated by partial deformation of the DNA double helix, although these are not stronger than the interactions between ssDNA and GO. We also examined its enzymatic digestion effects, molecular recognition, and biosensing at the dsDNA/GO interface. We believe these research efforts could improve understanding of the behavior of these GO/DNA entities, and thus facilitate applications in biosensors and bionanotechnology.

2. Results and Discussion

GO was first obtained by exfoliating graphite according to Hummer's method with slight modification (details seen in the Supporting Information).[16] Atomic force microscopy (AFM) images and the depth files (**Figure 1**a) demonstrate GO layers with thickness of 1.2 ± 0.2 nm. Such thickness is reasonable for oxygeneous graphene nanosheets, indicating single layer formation.[26] Interestingly, wrinkles on the GO with height about 2–10 nm were observed (Figure 1b), confirmed by high resolution transmission electron microscopy (HRTEM; Figure 1c).[16,17] It was calculated that natural wrinkles or ripples on graphene can stabilize the two-dimensional carbon structure with only one atom thickness.[28] We hypothesize that such wrinkles on GO have a similar role in flexible single-layer GO sheets. X-ray photoelectron spectroscopy (XPS) was also performed to characterize the oxygen-containing groups on GO (see Figure S1a in the Supporting Information), in which three different peaks centered at 285.6, 286.6, and 288.4 eV were observed, corresponding to C=O, C=O and O=C=O groups, respectively. The production of GO with high quality was also confirmed by FTIR and Raman spectra (see Figure S1b,c in Supporting Information).

In a typical experiment, dye-labeled ssDNA and dsDNA were used to investigate the interaction of DNA with GO (**Figure 2**).[22–24,27] Upon interacting with GO, Cy3-labeled ssDNA (Cy3-ssDNA) and dsDNA (Cy3-dsDNA) both exhibited substantially quenched fluorescence (Figure 2a). In 25 μg mL^{-1} GO, nearly 100% of the fluorescence of 20 nM Cy3-ssDNA could be quenched within 5 min, while only 30% was quenched for 20 nM dsDNA. These results correlate well with previous reports showing that dsDNA has a weaker or slower adsorption on GO.[17,18,22] Fluorescence titration experiments were performed to probe the quenching ability of Cy3-labeled DNA by GO (Figure S2, Supporting Information). Various amounts of GO were added into 20 nM Cy3-DNA solution. Interestingly, as more GO was added, the fluorescence of Cy3-dsDNA decreased gradually. When three-times this GO quantity (up to 75 μg mL^{-1}) was added, more than 90% fluorescence quenching was observed (Figure 2b). These results illustrate that a fluorescence resonance energy-transfer process happened

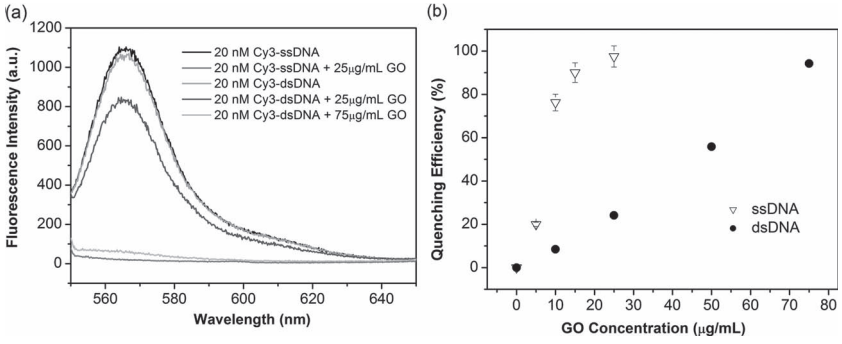

Figure 2. a) Fluorescence spectra of Cy3-ssDNA and Cy3-dsDNA before and after adding GO in 75 mM Tris–HCl buffer (pH 7.5). b) Fluorescence quenching efficiency as the function of Cy3-labeled ssDNA and dsDNA in terms of the different concentration of GO. Excitation wavelength: 490 nm. DNA concentrations: 20 nM.

between dye-labeled dsDNA and GO. In a control experiment the cyanine dye Cy3 was incubated with 75 μg mL^{-1} GO; the fluorescence results showed that less than 5% fluorescence was quenched (data not shown).[14,17] To further exclude the fluorophore adsorption effect on GO, label-free DNA with a common DNA-intercalating dye (SYBR Green I) was used (Figure S3, Supporting Information).[29] Noted that dsDNA (20 nM) showed much higher fluorescence than ssDNA (20 nM). Once GO (75 μg mL^{-1}) was added, both of ssDNA and dsDNA would be almost non-fluorescent. Furthermore, a long, more than 40000 bases natural λDNA was also studied and the results show an obvious fluorescence quenching in the presence of GO (Figure S4, Supporting Information), indicating that the longer dsDNA also show high binding affinity with GO.

Fluorescence quenching arose from the adsorption of DNA on GO and the approach of dyes to the GO surface. The fluorescence quenching was attributed to the electron or energy transfer between proximate Cy3 dye and GO surface.[17–20] Time-dependent studies reveal very fast assembly kinetics of ssDNA and dsDNA on GO. The fluorescence quenching efficiency [$(1 - F/F_0)$, where F_0 and F correspond to the fluorescence intensity before and after addition of GO, respectively] was 82% for ssDNA and 72% for dsDNA, within 300 s (Figure S5, Supporting Information). It should be noted that the quenching efficiency of ssDNA was slightly higher than that of dsDNA, which might be attributed to the fact that ssDNA is more flexible in conformation and the unpaired bases could closely interact with the graphene surface. Further measurements using fluorescence anisotropy (FA) confirmed the binding events of ssDNA and dsDNA to GO.[22] FA can differentiate the molecular weights of the fluorophore, which is commonly used to judge whether the DNA attaches on the surface or is in solution. As shown in Figure S6 (Supporting Information), the FAs of Cy3-labeled ssDNA and dsDNA were 0.059 and 0.088, respectively; upon addition of GO, those values changed to 0.441 and 0.387, respectively. These FA results confirmed the binding of ssDNA and dsDNA to GO. Therefore, the fluorescence results revealed that both ssDNA and dsDNA could interact with the GO surface, in spite of the different binding affinities.

All the above results demonstrate that DNA does interact with GO. It is well known that ssDNA closely interacts with GO mainly through π–π stacking interactions. However, little work has been undertaken to understand the mechanism of GO–dsDNA interactions. A previous report indicated that the presence of metal ions would dramatically increase the chance that dsDNA binds to GO.[24] So, salt-concentration dependency studies were first performed to explore the contribution of electrostatic interactions between dsDNA and GO. Interestingly, with the increase of Na^+ concentration from 40 to 400 mM, no obvious fluorescence change was observed for the mixture of dsDNA and GO (Figure S7, Supporting Information). This finding excluded electrostatic interactions as having a primary role in the interaction. According to a recently MD simulation,[25] graphene can severely deform a DNA segment and adsorb it on the carbon surface because of the breaking of the ending basepairs of the DNA duplex. The primary driving force is the π–π stacking interaction between the ending basepairs of DNA and the carbon rings. Nevertheless, there no experiment has been performed to illustrate this speculation to date.

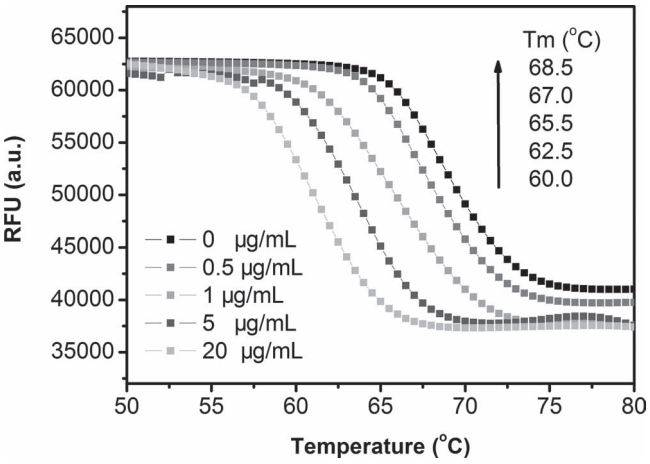

Figure 3. Melting profiles of DNA in the absence or presence of GO. From top to bottom: 0, 0.5, 1, 5, 20 μg mL^{-1} GO in 75 mM Tris-HCl buffer (pH 7.5) solution. SYBR Green I dye was used as the detection signal.

To get insight into this interaction of DNA duplex with GO, DNA melting transition analysis was conducted.[30] **Figure 3** shows the fluorescence melting profiles of DNA in the presence of GO. Note, the melting peak (T_m value) was obtained by plotting the negative first derivative of fluorescence ($-dRFU/dT$) against temperature (T). A decrease in T_m was observed with increasing GO concentration. The T_m of DNA was 68 °C without GO. After addition of GO, however, the melting curve results show that the T_m decreased gradually with the increase of the GO concentration. This finding suggests that GO influences the thermal stability of DNA and thereby reduce the T_m of the DNA fragments. In Figure 3, a lower fluorescence intensity with increasing GO concentration was also observed, which may be due to fluorescence quenching by GO.

To determine whether GO can affect DNA duplex stability, we compared circular dichroism (CD) spectra of DNA duplexes with different base pairs, varying from 5 to 25 bp, in the presence of GO. After forming a duplex, DNA was separately incubated with a designated concentration of GO solution for a long period of time (>12 h) at room temperature. As is known, duplex DNA presents a typical DNA spectrum with a positive peak at 275 nm and negative one at 246 nm (crossover point, 258 nm).[15] Thus, upon incubation with GO, both the intensities of the typical CD bands of dsDNA with 15 bp were monitored (**Figure 4**A). With increasing concentration of GO from 0 to 200 μg mL^{-1}, both the positive and negative band intensities decreased. Moreover, for the short-length DNA duplex, a significantly decrease in both the CD intensities of typical duplex bands were observed. In contrast, only a slight decrease of intensity occurred for the longer DNA duplex (Figure S8, Supporting Information). The intensities at 275 or 246 nm as a function of the concentration of different length DNA are summarized in Figure 4B. It is noted that the shorter the length of DNA duplex, the more the CD intensity decreases. For instance, the CD intensity of 5 bp DNA duplex decreased dramatically (nearly 60%) upon the addition of GO, indicating that most of duplexes were dissociated after incubation with GO.

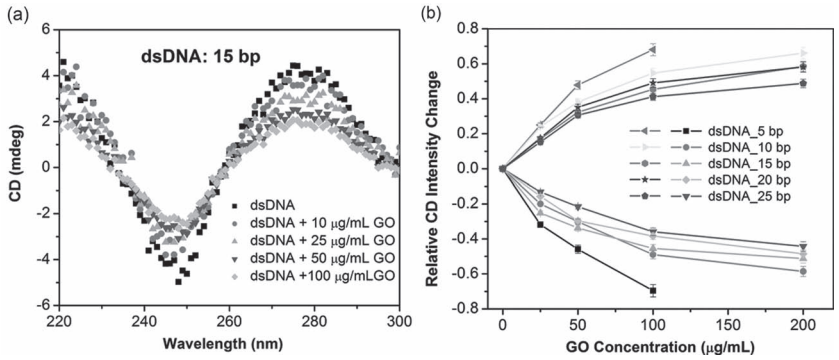

Figure 4. CD spectral changes of dsDNA induced by incubation with GO: a) CD spectra of dsDNA with 15 bp at 2 μM on adding different concentration of GO with incubation for 12 h at 4 °C in 75 mM Tris-HCl buffer (pH 7.5). b) Plot of CD intensity at the 275 nm (positive) or at 256 nm (negative) as a function of the incubation GO concentration. The data were adapted from Figure S8 in the Supporting Information. Relative CD intensity change was calculated as $(1 - \theta/\theta_0)$, where θ_0 and θ correspond to the CD intensity of dsDNA before and after incubation with GO, respectively.

In combination with fluorescence and melting results, we can conclude that GO could destabilize the DNA duplex, by partial dissociation of the short double helix. On the other hand, the results also demonstrate that GO binding did not disturb the higher-order DNA structures for the longer DNA, because the CD intensity decreased only slightly, and hardly any change for longer DNA was observed in the presence of GO. These results coincide well with previous MD calculations.[25]

Motivated by previous reports that DNA assembled on nanoparticles exhibits enhanced resistance to enzymatic cleavage,[22,31] we further studied the enzymatic cleavage of DNA duplex in the presence of GO. As described in **Figure 5**a, appreciable fluorescence quenching of dsDNA was observed in the presence of GO. However, on the introduction of DNA enzyme I the fluorescence of dsDNA/GO systems recovered remarkably (over 50%), implying that dsDNA assembled on GO could not be fully protected from enzymatic cleavage by DNA enzyme I. Two types of dsDNA-specific enzymes, restriction endonuclease EcoR I and Exo III, were further investigated. As shown in Figure 5b, no significant fluorescence recovery was observed after the hybridization between the bound ssDNA (P1) on GO and its complementary sequence, consistent with the aforementioned findings that dsDNA could bind to GO. However, the quenched fluorescence of dsDNA by GO was recovered substantially, up to 70%, after addition of restriction endonuclease EcoR I. Considering the fidelity of restriction endonuclease in specific cleavage of dsDNA, the observation of fluorescence recovery proves that the hybridization of ssDNA with its complementary on the GO surface was kept in its native duplex conformation and that the assembly on GO did not shield the dsDNA from the recognition by restriction endonuclease. The FA changes in DNA/GO systems prove to be very sensitive to enzyme digestion, which can be used as a powerful tool to monitor enzyme digestion.[22] So, EcoR I enzymatic cleavage of dsDNA was further confirmed by significant FA changes after cleavage. After the cleavage, FA decreased dramatically because more dye molecules were released from the GO surface.[22] However, after incubating Exo III with different concentration dsDNA in the presence of GO, no fluorescence recovery was observed (**Figure 6**a). FA detection further confirms the resistance to Exo III degradation and no significant FA change was observed for dsDNA after incubation with Exo III, which is quite different from EcoR I cleavage (Figure 6b). FA measurements for EcoR I and Exo III clearly demonstrate their differences in digesting dsDNA/GO systems.

The different responses of bound dsDNA on GO to EcoR I and Exo III are shown schematically in **Scheme 1**. Our above study has illustrated that partial deformation of duplex DNA happened when interacting with GO. For the different cleavage effect, one possible reason is that the conformational change of dsDNA helix may influence the enzymatic activity. On the other hand, according to previous reports, the enzyme cleavage inhibition in the nanoparticle system was induced by steric effect of nanomaterials, achieving a high affinity in the adaptive binding event.[31,32] For example, SWNTs can be attracted to the major groove sites of the DNA duplex under certain conditions, which was confirmed by experiments and simulations.[33] Therefore, it is also probably that strong binding of dsDNA to GO results in great steric hindrance for Exo III.[27] The enzymatic responses of DNA on two-dimensional GO with one atom thickness have not been reported so far and need further investigations for their potential in bionanoelectronic or biological applications.

3. Conclusions

We experimentally investigated the interactions of DNA/GO as well as its biological enzyme digestion effect. A deeper understanding of the interaction of the duplex DNA with GO has been

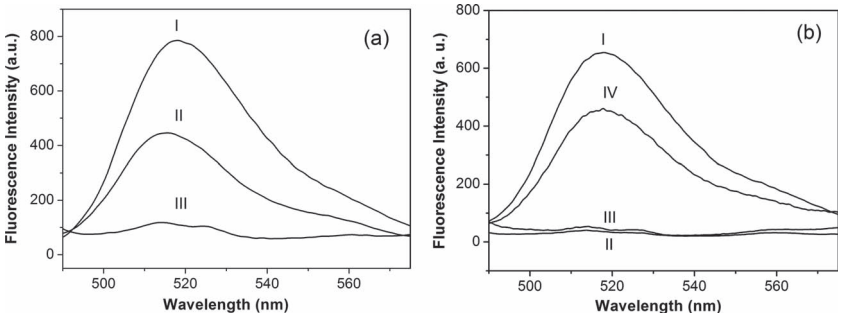

Figure 5. Specific enzymatic cleavage effect of dsDNA on GO: a) fluorescence responses for P2-dsDNA (I) in the sequential addition of GO (II), and DNA enzyme I (III). b) Fluorescence responses for P1-ssDNA (I) in the sequential addition of GO (II), target DNA (cDNA) (III) and EcoR I (IV). Concentration of DNAs: 20 nM; buffer: 25 mM Tris–HCl buffer (pH 7.5) for DNA enzyme I, 50 mM Tris–HCl buffer (pH 7.5) for EcoR I and Exo III; excitation wavelength: 470 nm.

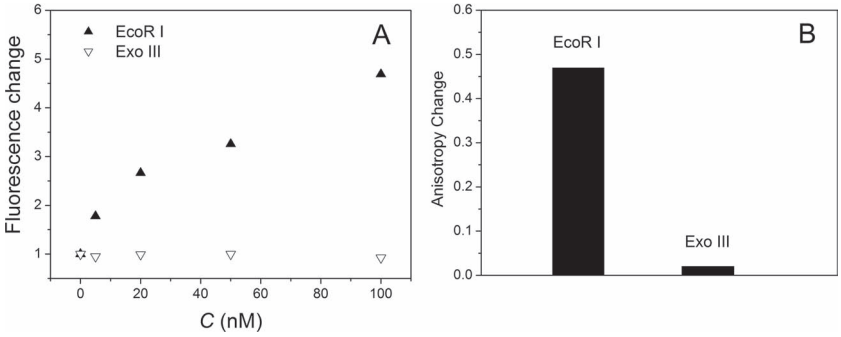

Figure 6. Enzymatic cleavage difference of EcoR I (▲) and Exo III (▽) for dsDNA on GO surface. a) Relative fluorescence intensity via added target DNA concentrations in the presence of EcoR I and Exo III, respectively. Relative fluorescence intensity was calculated as the fluorescence intensity ratio F/F_0, where F_0 and F correspond to the fluorescence intensity of ssDNA on GO before and after addition of targets and cleavage enzymes, respectively. b) Fluorescence anisotropy changes after enzymatic cleavage in the presence of 100 nM targets for ssDNA on GO. ssDNA concentration: 20 nM; excitation wavelength: 470 nm.

obtained. Our findings suggest for the first time that GO could adsorb DNA duplex, facilitated by a partial deformation of the double helix on the GO surface. In combination with previous MD simulations,[25] the possible primary driving force could be π-stacking interactions between the ending basepairs of DNA and the carbon rings. The binding affinity of dsDNA to GO may also be enhanced by hydrogen-bond formation between oxygenous groups of GO and DNA bases.[13,16,18,25] As an initiative to understand the bioeffect of GO/dsDNA interface, the enzymatic degradation of DNA duplexes on GO was investigaed, showing that DNA/GO could be effectively cleaved by DNA enzyme I and restriction endonucleases as EcoR I, while being highly resistant to the degradation by Exo III. Based on the specific fluorescence recovery of dsDNA assembled on graphene by restriction endonucleases, fluorescent biosensors could be constructed via target-mediated formation of specifically encoded dsDNA.[34] The unusual noncovalent assembly of dsDNA on the graphene is envisioned to have potential for diverse future applications, such as biological imaging, material science, sensing, and biomedicine.

4. Experimental Section

Materials: Graphite powder (99.99995%, 325 mesh) was purchased from Alfa Aesar. Other chemicals, $KMnO_4$, NaOH, KCl, and NaCl, were from Beijing Chemical Company. λDNA was purchased from Dingguo company (Beijing, China). SYBR Green I dye (Sigma S9430) was supplied at 10 000× concentration in DMSO. It was stored in 10 µL aliquots at −80 °C, and a working dilution of 50× solution in water was stored as multiple aliquots at −20 °C. Each aliquot of working dilution was discarded after a single use. All other chemicals were of analytical grade and obtained from Sinopharm Chemical Reagent Co. Ltd. The solutions were prepared using ultrapure water, which was obtained through a Millipore Milli-Q water purification system (Billerica, MA, USA) and had an electric resistivity >18.3 MΩ cm. The oligonucleotides used in this work were synthesized from Invitrogen Co. Ltd. (Shanghai, China). The thermodynamic parameters of all oligonucleotides were calculated using bioinformatics software (http://www.bioin-fo.rpi.edu/applications/), and no particular secondary structure was found for the synthesized oligonucleotide sequences. The sequences of the synthesized oligonucleotides used in the study the DNA/GO interrelations are given in Table S1 (see the Supporting Information). EcoR I was from Toyobo Co. (Japan) and Exonuclease III was bought from New England Biolabs (NEB, USA). DNA enzyme I was from Dingguo Biotech (Beijing, China).

Synthesis of Graphene Oxide (GO): Pre-oxidized graphite was re-oxidized by Hummers' method. Pretreated graphite powder was put into 0 °C concentrated H_2SO_4 (120 mL). Then, $KMnO_4$ (15 g) was added gradually under stirring and the temperature of the mixture was kept to be below 20 °C using an ice bath. Successively, the mixture was stirred at 35 °C for 4 h, and then diluted with deionized water (250 mL) keeping the temperature under 50 °C. Water (700 mL) was then injected into the mixture followed by adding H_2O_2 (30 wt-%; 20 mL) drop by drop. The mixture was filtered and washed with HCl aqueous solution (1 L) to remove metal ions followed by deionized water to remove the acid. The resulting solid was dried in air and diluted to make GO dispersion (0.5 wt-%). Finally, it was

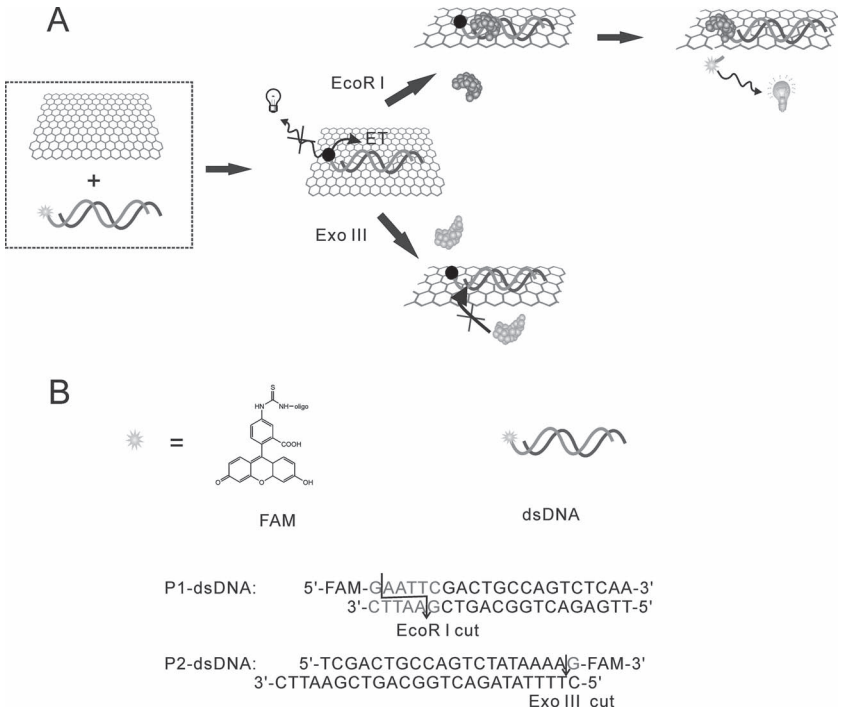

Scheme 1. Schematic illustration of dye-labeled dsDNA assembly on graphene oxide with unusual enzymatic cleavage effect. a) Schematic demonstration. Upon interacting with graphene, dye-labeled dsDNA shows quenched fluorescence. Restriction endonuclease EcoR I can cleave the assembled dsDNA, resulting in a recovery of fluorescence due to much weak adsorption of dye-labeled nucleotide on graphene, while the bound dsDNA is highly resisted to the degradation of Exo III with no fluorescence recovery. b) DNA sequence and FAM dye structure. The red part in the DNA sequences represents the cleavage sites of EcoR I and Exo III.

purified by dialysis for 1 week to remove the remaining metal species. Exfoliation was carried out by sonicating GO dispersion (0.1 mg mL^{-1}) under ambient condition for 1 h.

Characterization: The transmission electron microscope (TEM) images were obtained with a Hitachi model H-800 transmission electron microscope opened at an accelerating voltage of 100 kV. The samples mixing with ethanol (5 μL) were dropped on a Cu grid and left to dry in air condition for 10 h. Raman spectra were obtained using a confocal microprobe Raman system (Renishaw, RM2000).

For AFM characterization, typically, a sample for AFM imaging was prepared by first treating a freshly cleaved mica surface with 1 M $MgCl_2$ for 1 min, followed by addition of a sample solution (10 μL) onto the mica surface. The mica substrate was tilted to allow the droplet to spread on the surface. After adsorption for 1 min, the mica surface was washed twice with double-distilled water and dried with compressed air. The sample was then scanned in tapping mode with a Nanoscope III, Digital Instrument atomic force microscope.

Fluorescence measurements were conducted using an F-7000 Hitachi spectrometer, and fluorescence anisotropy was measured by FL3-P-TCSPC (JobinYvon, France). In a typical experiment, GO was added to dye-lableld ssDNA or dsDNA (20 nM) in Tris–HCl buffer (50 mM, pH 7.5) with NaCl (100 mM), Mg^{2+} (10 mM), and DTT (1 mM),. In the EcoR I cleavage studies, P1-ssDNA (20 nM) solution was sequentially incubated with GO, different concentration and EcoR I (200 U) at 37 °C. The EcoR I cleavage buffer (Toyobo, Japan) was Tris-HCl buffer (50 mM, pH 7.5) with NaCl (100 mM), Mg^{2+} (10 mM), and DTT (1 mM). Similarly with the EcoR I cleavage studies, P2-ssDNA (20 nM) was sequentially incubated with GO, different concentration T2 targets and Exo III (200 U) at 37 °C. The Exo III buffer (NEB, USA) was Tris-HCl buffer (10 mM) with Mg^{2+} (10 mM), and DTT (1 mM). DNA enzyme I cleavage was conducted in Tris-HCl buffer (25 mM, pH 7.5) with NaCl (50 mM), Mg^{2+} (5 mM), and DTT (0.5 mM), with DNA enzyme I (100–400 U). Generally the cleavage time for three enzymes was about 2 h, but in some cases cleavage time was as long as 20 h to maximize the cleavage.

Circular dichroism (CD) measurements were taken with a JASCO J-715 spectrometer with temperature control (JASCO International Co. Ltd., Tokyo, Japan) at room temperature unless otherwise specified. Samples were freshly prepared. DI water was used in the dialysis step instead of buffer.

Melting experiments were measured on a JPrism-7000 PCR equipped with a Chromo4 real-time fluorescence detector. The fluorescent agent SYBR Green I can emit fluorescent light when randomly intercalated into the minor groove of dsDNA and was used to monitor the production of double-stranded PCR products. Each reaction mixture (20 μL) contained DNA (1 μM), SYBR Green I (×10 000) and different concentration of GO solution (0–20 μg mL^{-1}).

Supporting Information

Supporting Information is available from the Wiley Online Library or from the author.

Acknowledgements

L.H.T. and H.X.C. contributed equally to this work. This work was financially supported by the National Basic Research Program of China (No. 2011CB935704), the National Natural Science Foundation of China (No. 20975060, No. 21005046), and Tsinghua University Initiative Scientific Research Program. L.H.T. gratefully acknowledges financial support from the China Scholarship Council. The authors thank Dr. J. S. Cheng for providing the graphene oxide samples and Prof. J. H. Jiang from Hunan University and Z. Wang from UIUC for their professional advice.

Received: November 29, 2011
Revised: February 7, 2012
Published online: April 23, 2012

[1] C. M. Niemeyer, *Angew. Chem. Int. Ed.* **2001**, *40*, 4128.
[2] D. J. Maxwell, J. R. Taylor, *J. Am. Chem. Soc.* **2002**, *124*, 9606.
[3] J. Liu, Z. Cao, Y. Lu, *Chem. Rev.* **2009**, *109*, 1948.
[4] E. Katz, I. Willner, *ChemPhysChem* **2004**, *5*, 1084.
[5] Z. Wu, Z. Zhen, J. H. Jiang, G. L. Shen, R. Q. Yu, *J. Am. Chem. Soc.* **2009**, *131*, 12325.
[6] M. E. Hughes, E. Brandin, J. A. Golovchenko, *Nano Lett.* **2007**, *7*, 1191.
[7] M. Zheng, A. Jagota, M. S. Strano, A. P. Santos, P. Barone, S. G. Chou, B. A. Diner, M. S. Dresselhaus, R. S. Mclean, G. B. Onoa, *Science* **2003**, *302*, 1545.
[8] C. Zhao, K. Qu, C. Xu, J. Ren, X. Qu, *Nucleic Acids Res.* **2011**, *39*, 3939.
[9] N. W. S. Kam, M. O'Connell, J. A. Wisdom, H. Dai, *Proc. Natl. Acad. Sci. USA* **2005**, *102*, 11600.
[10] R. Yang, Z. Tang, J. Yan, H. Kang, Y. Kim, Z. Zhu, W. Tan, *Anal. Chem.* **2008**, *80*, 7408.
[11] K. S. Novoselov, A. K. Geim, S. V. Morozov, D. Jiang, Y. Zhang, S. V. Dubonos, I. V. Grigorieva, A. A. Firsov, *Science* **2004**, *306*, 666.
[12] M. J. Allen, V. C. Tung, R. B. Kaner, *Chem. Rev.* **2009**, *110*, 132.
[13] L. Tang, Y. Wang, Y. Li, H. Feng, J. Lu, J. H. Li, *Adv. Funct. Mater.* **2009**, *19*, 2782.
[14] Y. Wang, Z. Li, D. Hu, C. T. Lin, J. H. Li, Y. Lin, *J. Am. Chem. Soc.* **2011**, *132*, 9274.
[15] A. J. Patil, J. L. Vickery, T. B. Scott, S. Mann, *Adv. Mater.* **2009**, *21*, 3159.
[16] L. Tang, Y. Wang, Y. Liu, J. H. Li, *ACS Nano* **2011**, *5*, 3817.
[17] L. Lin, Y. Liu, X. Zhao, J. H. Li, *Anal. Chem.* **2011**, *83*, 8396.
[18] H. Chang, L. Tang, Y. Wang, J. Jiang, J. H. Li, *Anal. Chem.* **2010**, *82*, 2341.
[19] S. He, B. Song, D. Li, C. Zhu, W. Qi, Y. Wen, L. Wang, S. Song, H. Fang, C. H. Fan, *Adv. Funct. Mater.* **2010**, *20*, 453.
[20] M. Wu, R. Kempaiah, P. J. J. Huang, V. Maheshwari, J. Liu, *Langmuir* **2011**, *27*, 2731.
[21] Z. Liu, J. T. Robinson, X. Sun, H. Dai, *J. Am. Chem. Soc.* **2008**, *130*, 10876.
[22] Z. Tang, H. Wu, J. R. Cort, G. W. Buchko, Y. Zhang, Y. Shao, I. A. Aksay, J. Liu, Y. Lin, *Small* **2010**, *6*, 1205.
[23] D. Umadevi, G. N. Sastry, *J. Phys. Chem. Lett.* **2011**, *2*, 1572.
[24] H. Lei, L. Mi, X. Zhou, J. Chen, J. Hu, S. Guo, Y. Zhang, *Nanoscale* **2011**, *3*, 3888.
[25] X. Zhao, *J. Phys. Chem. C* **2011**, *115*, 6181.
[26] C. Gmez-Navarro, R. T. Weitz, A. M. Bittner, M. Scolari, A. Mews, M. Burghard, K. Kern, *Nano Lett.* **2007**, *7*, 3499.
[27] N. Mohanty, V. Berry, *Nano Lett.* **2008**, *8*, 4469.
[28] J. C. Meyer, A. K. Geim, M. I. Katsnelson, K. S. Novoselov, T. J. Booth, S. T Roth, *Nature* **2007**, *446*, 60.
[29] R. S. Swathi, K. L. Sebastiana, *J. Chem. Phys.* **2008**, *129*, 054703.
[30] Y. Liang, F. Luo, Y. Lin, Q. Zhou, G. Jiang, *Carbon* **2009**, *47*, 1457.
[31] X. X. He, K. Wang, W. Tan, B. Liu, X. Lin, C. He, D. Li, S. Huang, J. Li, *J. Am. Chem. Soc.* **2003**, *125*, 7168.
[32] N. L. Rosi, D. A. Giljohann, C. S. Thaxton, A. K. R. Lytton-Jean, M. S. Han, C. A. Mirkin, *Science* **2006**, *312*, 1027.
[33] G. Lu, P. Maragakis, E. Kaxiras, *Nano Lett.* **2005**, *5*, 897.
[34] S. Nakayama, L. Yan, H. O. Sintim, *J. Am. Chem. Soc.* **2008**, *130*, 12560.